	Experiment title: GIXRD characterization of InGaN quantum dot overgrowth	**Experiment number:** HS-4148
Beamline: ID32	**Date of experiment:** from: 10-Mar-2010 to: 17-Mar-2010	**Date of report** 31-Aug-2010
Shifts: 18	**Local contact(s):** Jérôme Roy	*Received at* ESRF:
Names and affiliations of applicants (* indicates experimentalists): Th. Schmidt*, S. Figge, S. Kuhr*, T. Wilkens*, Institute of Solid State Physics, University of Bremen, Germany		

Experimental Report

1. Background and objectives

A two-step growth procedure has been developed at our institute that permits the fabrication of light-emitting devices based on InGaN quantum dots embedded in GaN. The optical properties of such structures have been demonstrated to show clear signatures of true quantum-dot emission [1, 2]. The growth is performed by metal organic vapor phase epitaxy (MOVPE) on wurtzite GaN(0001) template layers. The procedure consists of a first step in which an $In_xGa_{1-x}N$ layer with a high In concentration x, a so-called nucleation layer, is deposited onto the GaN substrate at a relatively low temperature of about 600 °C. Owing to the miscibility gap of InGaN, this results in spinodal decomposition into a phase with a very high In concentration and a low-concentration phase, as has been proven in a previous experiment (HS-3781). In the second growth step, the nucleation layer is overgrown with a pure GaN layer or an $In_yGa_{1-y}N$ layer with very low y at a significantly higher temperature of about 800 °C or above.

The aim of this study was to characterize structural properties like the strain state and the chemical composition of the InGaN phases of the nucleation layer in dependence on the average In content (more precisely: on the In/(In+Ga) precursor flux ratio η) as well the development of these properties during subsequent temperature raise and GaN overgrowth. For this purpose, two series of samples were investigated. The samples of the first series were quenched immediately after deposition of the formation layer which was grown at 600 °C with $\eta = 0.73$, $\eta = 0.82$, and $\eta = 1.00$, respectively. For the second series, $\eta = 0.82$ was used for all samples, but different annealing procedures were applied: (i) no annealing, (ii) annealing at the growth temperature (600 °C) for 4 minutes, (iii) annealing for 4 minutes while ramping the temperature to 750 °C, and (iv) 4 minutes annealing while ramping to 750 °C, followed by 44 nm cap layer growth and simultaneous stepwise temperature raise to 1050 °C.

2. Results

Grazing-incidence x-ray diffraction measurements were carried out in a z-axis geometry setup with a fixed incident angle of 0.5°, i. e. well above the critical angle for total external reflection. Unfortunately, the position-sensitive detector requested in the proposal was not avaible and a point detector was used instead. This turned out to severely limit the amount of data that could be acquired during the allocated beamtime. Measurements

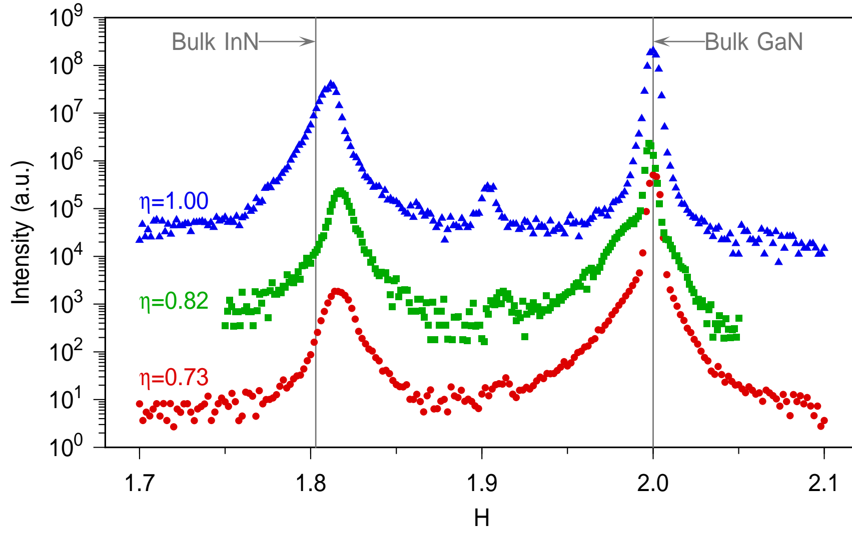

Figure 1: H-scans in the vicinity of the (200) reflection for nucleation layers grown with different In/(In+Ga) precursor flux ratios η.

at both in-plane reflections (i. e. with $L \approx 0$) as well as at out-of-plane reflections were performed, the latter allowing to also determine the vertical lattice constant of the different InGaN phases.

Fig. 1 shows radial scans of the (200) in-plane reflection for the first sample series. For the flux ratios used here, the profiles show similar characteristics. The GaN (200) reflection exhibits a shoulder towards smaller H values which is attributed to an In-depleted InGaN phase. This is most prominent for $\eta = 0.82$. For $\eta = 0.73$, the shoulder is broader, corresponding to laterally smaller domains. For $\eta = 1.00$, the GaN(200) spot looks almost symmetric, which suggests that for a pure InN precursor flux only very little InGaN with low In content is formed. In all GIXRD profiles depicted in Fig. 1, a strong signal at $H \approx 1.8$ is observed that is attributed to an In-rich phase. From its position, it can already be deduced that this phase consist of almost pure InN. With increasing In flux ratio, this peak tends to shift to the left, indicating a slightly increasing In content in the In-rich phase. In addition, a small peak between the InN and the GaN Bragg spot is seen at $H \approx 1.9$. This could either be explained by the presence of an additional In phase with about 50 % In content (which is rather unlikely due to the InGaN miscibility gap) or by periodic misfit dislocations at the interface between the substrate and the In-rich regions. Such a misfit dislocation array would lead to one satellite spot between the two Bragg spots for this second order reflection [3, 4]. The latter scheme could in principle be verfied by similar scans at the (300) reflection, where two satellites are expected between the two Bragg peaks. Unfortunately, this was not possible in our setup due to polarization effects.

Reciprocal-space maps recorded near the (203) reflection are shown for the first sample series in Fig. 2. The spot related to the In-rich phase is clearly separated from the GaN reflection both in lateral (H) as well as in vertical (L) direction. The inclined shape of this InN spot points to a distribution of strain inside these In-rich islands, which have a three-dimensional morphology, as can be deduced from the widths of this peak along H and L.

Near the GaN crystal truncation rod (CTR), again a shoulder can be seen which extends towards lower H and lower L values, best to be seen for $\eta = 0.82$. This is again attributed to an In-depleted phase. This phase has a smaller average thickness in real-space, as the shuolder is extended along the L-direction. For $\eta = 1.00$, no clear indication for such a shoulder is visible, again pointing to only very small amounts of In-depleted material. Line scans along the GaN (20) CTR are shown in Fig. 3. An In-depleted phase shows up as a pronounced shoulder for $\eta = 0.73$, whereas the rather smooth tails observed for $\eta = 1.00$ seem to originate from the wetting layer only.

From our data, the vertical and the lateral lattice constant of the In-rich phase have been determined, allowing for the analysis [5] of the average In content x as well as the average degree of relaxation R, based on Vegard's law. The results are shown in the upper half of Table 1. For all In flux ratios used here, the In-rich phase is almost completely relaxed. The In content slightly increases from about 95 % to about 99 % with increasing η.

The impact of annealing and overgrowth is demonstrated in the radial in-plane scans near the (200) reflection in

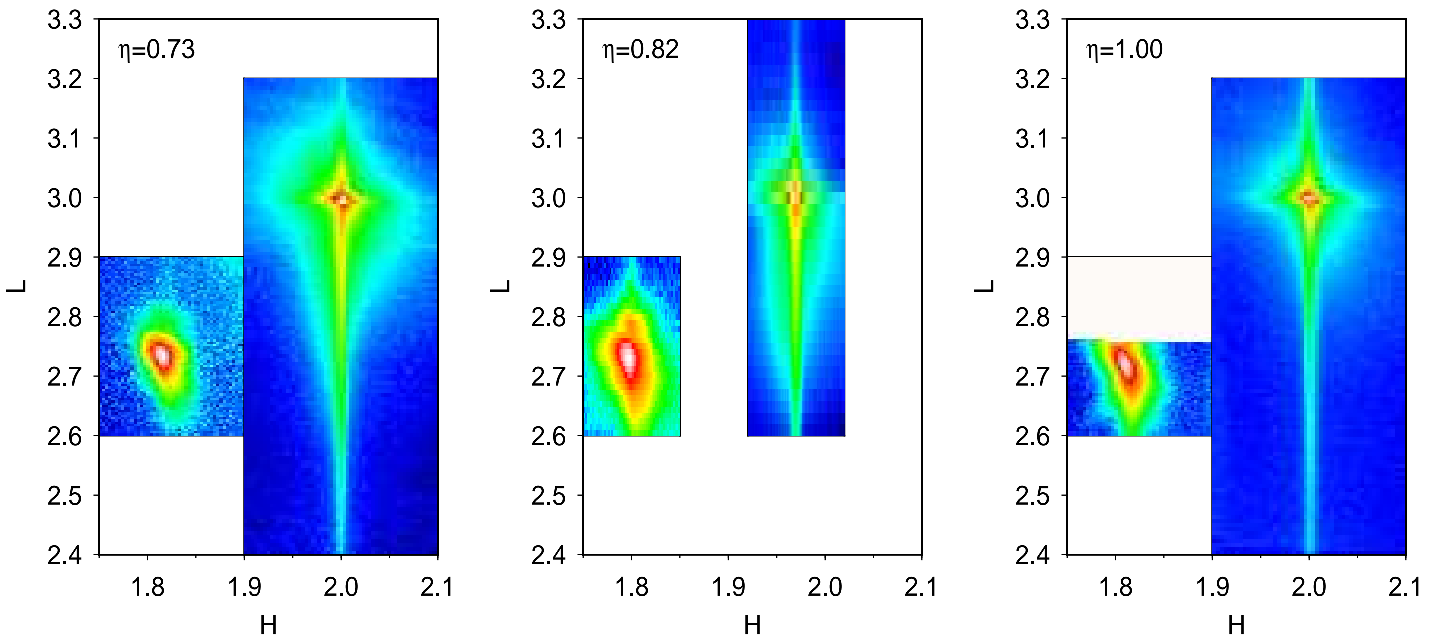

Figure 2: Reciprocal space maps in the H-L plane near the (203) reflection for nucleation layers grown with different In/(In+Ga) precursor flux ratios η.

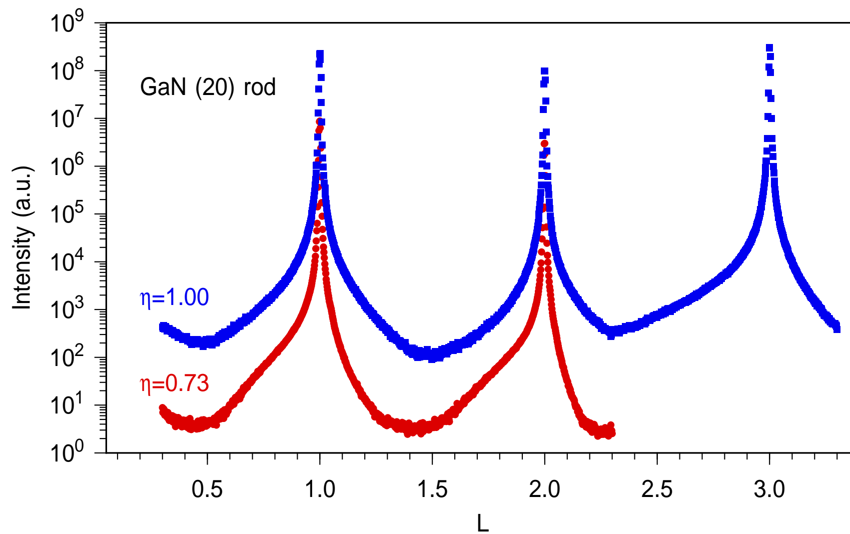

Figure 3: L-scans along the GaN (20) substrate crystal truncation rod for nucleation layers grown with different In/(In+Ga) precursor flux ratios η.

Fig. 4. Compared to the sample for which the temperature was quenched immediately after nucleaction layer growth, subsequent annealing leads to a reduced signal from the In-depleted phase. For annealing at 600 °C, the peak related to the In-depleted phase shifts towards the GaN peak, pointing to a further reduction of the In concentration in this phase. For an annealing temperature of 750 °C, a signature from the In-depleted phase can hardly be identified at all. Simultaneously, the peak corresponding to the In-rich phase shifts slightly towards higher H-values. These findings indicate that during annealing the total In content of the layer is reduced. Whereas the In-rich regions are only slightly affected, the In-depleted phases seem to dissolve more or less completely at 750 °C. A drastic change is found after cap layer growth, where no signal from an In-rich phase is observed (see upper curve in Fig. 4). Nevertheless, the GaN(200) reflection looks wider and asymmetric after cap layer growth again, with a larger tail towards lower H values. Apparently, the In-rich phases have dissolved and small domains with lower In concentration have formed which might be attributed to quantum dots.

These findings are confirmed from measurements at out-of-plane reflections, such as shown in the reciprocal-space maps in Fig. 5. Again, the position of Bragg spot related to the In-rich phase has been used for a quantitative analysis of the mean strain state and composition. The results are listed in the lower half of Table 1. Whereas

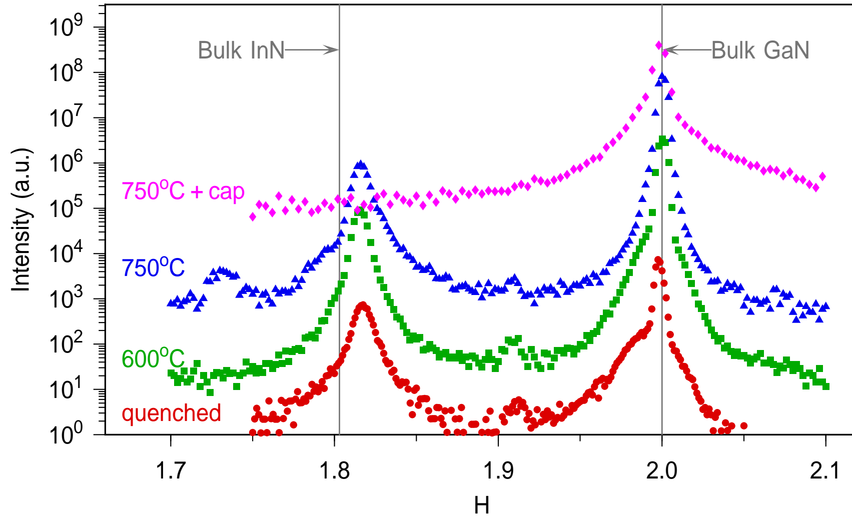

Figure 4: H-scans in the vicinity of the (200) reflection for $\eta = 0.82$ and different annealing conditions.

annealing at the growth temperature has no measurable effect as compared to no annealing, an increase of the annealing temperature to 750 °C slightly reduces the In content of the In-rich phase.

3. Conclusion and outlook

The influence of the In precursor flux on the strain state and composition of the nucleation layer in the two-step growth of InGaN quantum dots has been investigated, as well as the impact of subsequent annealing which is necessary for overgrowth in this two-step growth approach. Spinodal decomposition into an In-rich phase and an In-depleted phase has been confirmed. The development of the strain state and composition of the In-rich phase has quantitatively been determined. A corresponding analysis of the In-depleted phase from our data, as well as the determination of morphological parameters like island widths and heights is still under way. Regarding the In-depleted phase, the analysis is challenging, partly because of the close vicinity of the corresponding diffraction signal to the quite strong substrate signal, and partly because of the relatively low density of data points which is owed to the detector system used.

With a position sensitive detector, a much higher density of data points can be achieved, allowing even three-dimensional reciprocal-space mapping. Moreover, with a position sensitive detector it should be possible to perform reciprocal space mapping under different incident angles in reasonable time, which would allow to obtain depth information and also to suppress the relatively strong substrate signal at low incident angles in order to reliably investigate the evolution of the In-depleted phase and thus to get a deeper insight into the processes leading to quantum dot formation. For the latter purpose, it would be interesting to investigate the cap layer growth, which has been shown to have a dramatic impact, in more detail. Therefore, similar experiments for different cap layer thicknesses, with an emphasis on the initial stages of overgrowth, should be performed.

Table 1: Relative lateral Bragg spot position $H_{\mathrm{InN}}/H_{\mathrm{GaN}}$ and vertical Bragg spot position $L_{\mathrm{InN}}/L_{\mathrm{GaN}}$ of the In-rich phase, as well as In concentration x and degree of relaxation R derived from these Bragg spot positions, as a function of the In/(In+Ga) precursor flux ratio η and of the annealing conditions.

η	annealing	$H_{\mathrm{InN}}/H_{\mathrm{GaN}}$	$L_{\mathrm{InN}}/L_{\mathrm{GaN}}$	x	R
0.73	quenched	0.9075	0.9119	0.951	0.981
0.82	quenched	0.9077	0.9102	0.960	0.969
1.00	quenched	0.9050	0.9079	0.989	0.972
0.82	quenched	0.9075	0.9119	0.951	0.981
0.82	600 °C	0.9073	0.9118	0.952	0.982
0.82	750 °C	0.9079	0.9128	0.943	0.985
0.82	750 °C+cap	—	—	—	—

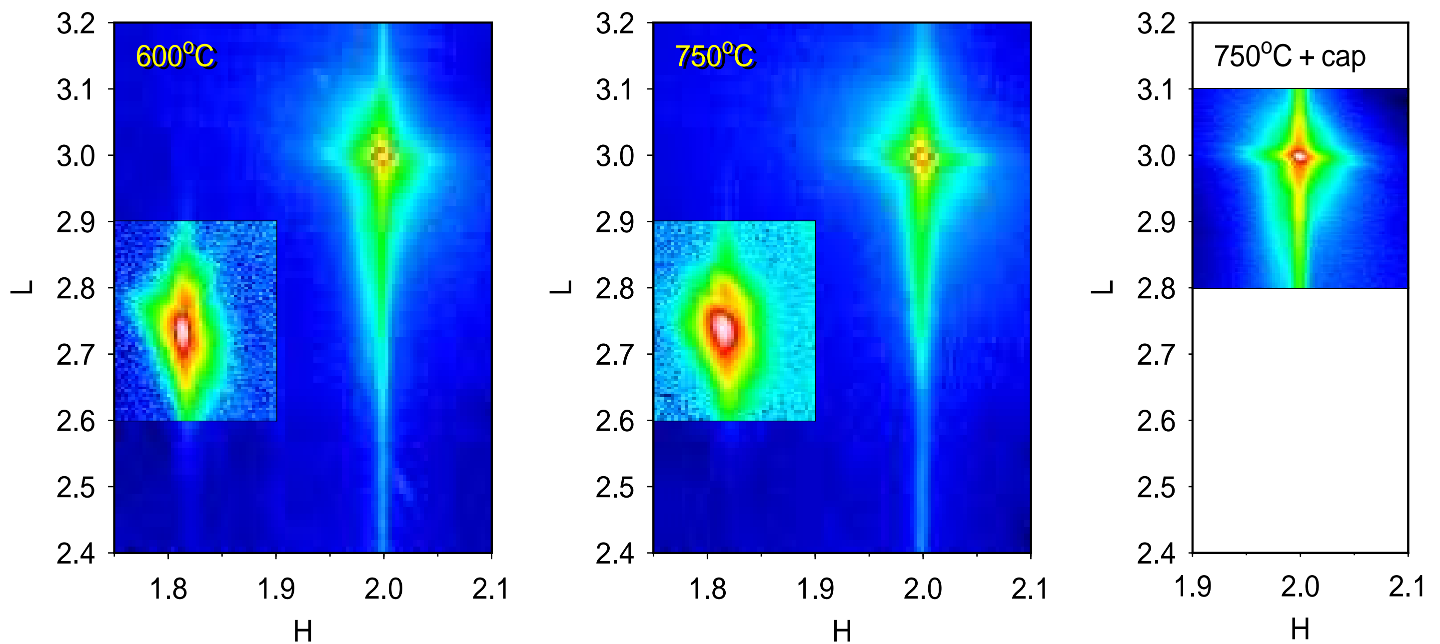

Figure 5: Reciprocal space maps in the H-L plane near the (203) reflection for $\eta = 0.82$ and different annealing conditions.

4. References

[1] T. Yamaguchi, K. Sebald, H. Lohmeyer, S. Gangopadhyay, J. Falta, J. Gutowski, S. Figge, and D. Hommel, phys. stat. sol. (c) **3**, 3955 (2006).

[2] J. Kalden, C. Tessarek, K. Sebald, S. Figge, C. Kruse, D. Hommel, and J. Gutowski, phys. stat. sol. (a) **207**, 1428 (2010).

[3] Th. Schmidt, R. Kröger, T. Clausen, J. Falta, A. Janzen, M. Kammler, P. Kury, P. Zahl, and M. Horn-von Hoegen, Appl. Phys. Lett. **86**, 111910 (2005).

[4] Th. Schmidt, R. Kröger, J. I. Flege, T. Clausen, J. Falta, A. Janzen, P. Zahl, P. Kury, M. Kammler, and M. Horn-von Hoegen, Phys. Rev. Lett. **96**, 066101 (2006).

[5] Th. Schmidt, J. I. Flege, M. Siebert, S. Figge, T. Yamaguchi, D. Hommel, and J. Falta, phys. stat. sol. (c) **6**, S602 (2009).